1284 Russian Chemical Bulletin, International Edition, Vol. 69, No. 7, pp. 1284—1289, July, 2020

Synthesis of magnetic hybrid magnetite—gold nanoparticles*

S. V. Saikova,[a,b]★ T. V. Trofimova,[a] A. Yu. Pavlikov,[a] D. V. Karpov,[a] D. I. Chistyakov,[a] and Yu. L. Mikhlin[b]

[a]Siberian Federal University,
79 Svobodny prosp., 660041 Krasnoyarsk, Russian Federation.
E-mail: ssai@mail.ru
[b]Institute of Chemistry and Chemical Technology, Siberian Branch of the Russian Academy of Sciences,
Federal Research Center "Krasnoyarsk Science Center of the Siberian Branch of the Russian Academy of Sciences",
Build. 24, 50 ul. Akademgorodok, 660036 Krasnoyarsk, Russian Federation.
E-mail: yumikh@icct.ru

Methods for the synthesis of hybrid nanoparticles, consisting in the simultaneous modification of the magnetic core and reduction of gold on the surface using various reagents, were proposed and developed. Depending on synthesis conditions, various hybrid nanoparticles were obtained, namely, hybrid nanoparticles decorated with gold nuclei and hybrid nanoparticles of the core—shell type. The obtained products can be used as promising materials for catalytic and biomedical applications.

Key words: hybrid nanoparticles, magnetite, gold, core—shell structure.

The synthesis of nanoparticles (NPs) with unique properties is an area of priority for the development of modern nanotechnology. The interest directed toward these materials is primarily related to their use in various fields of science and technology: chemistry, physics, biology, microelectronics, medicine, and biotechnology.[1—4] Researchers are particularly interested in magnetic hybrid NPs based on oxide materials, which can potentially be used in medicine. These particles can interact with high-frequency electromagnetic radiation, therefore, they are used as contrast agents for magnetic resonance imaging,[2] as well as in cancer thermotherapy.[3] The use of magnetic NPs as vectors for the targeted delivery of drugs and diagnostic substances is of particular interest. These particles along with drug molecules located on their surface can be easily directed toward specific organs and tissues using an external magnetic field.

A convenient magnetic material for these purposes is magnetite, the nanoparticles of which are the most studied.[5,6] Colloidal magnetite solutions can be obtained without the use of sophisticated equipment and lengthy high-temperature annealing procedures.[7] At the same time, when using magnetite NPs, their chemical lability presents a problem. In addition, many works[8—10] have been devoted to the study of the cytotoxicity of Fe_3O_4 nanoparticles. The use of non-functionalized magnetite NPs causes ferroptosis of cells in cultures and damage to various organs and tissues in animals. Hybrid magnetite NPs which are coated with an inert shell lack this drawback. In this case, the toxicological effect of magnetite is reduced since it does not interact with the environment. When a noble metal, for example, gold, is used as a shell, NPs acquire the ability to absorb optical and IR radiation due to surface plasmon resonance (SPR). This property of hybrid NPs can be used in cancer thermotherapy.[11] It should be noted that the methods of obtaining hybrid structures based on magnetite and gold described in published literature are characterized by low reproducibility, while commercially available drugs announced as containing hybrid NPs are revealed to be simple mixtures of magnetite and gold nanoparticles upon detailed study.

The goal of this work is to develop a method for the synthesis of hybrid nanoparticles based on magnetite and gold and their characterization.

Experimental

Magnetite samples with different particle sizes, which were obtained by two different methods (Mag-1 and Mag-2), were used in this work. All the reagents used for the synthesis were classified as reagent grade or analytical grade and did not undergo further purification. In order to prevent the oxidation of iron(II), the water used for the experiment was refluxed for 1 h to reduce the concentration of oxygen dissolved in it.

Synthesis of sample Mag-1.[7] A mixture of $FeCl_3 \cdot 6H_2O$ (0.55 g) and $FeCl_2 \cdot 7H_2O$ (1.01 g) (Aldrich, USA) with a molar ratio of 1 : 2 dissolved in water (55 mL) was added to a 6 *M* NaOH solution (100 mL) with continuous stirring on a magnetic stirrer under inert nitrogen atmosphere (bubbling rate ~60 bubbles per

---

* Based on the materials of the XXI Mendeleev Congress on General and Applied Chemistry (September 9—13, 2019, St. Petersburg, Russia).

Published in Russian in *Izvestiya Akademii Nauk. Seriya Khimicheskaya,* No. 7, pp. 1284—1289, July, 2020.

1066-5285/20/6907-1284 © 2020 Springer Science+Business Media LLC

min), the mixture was maintained at 60 °C with stirring for 1 h. After being allowed to stand for 1 h, the precipitate was isolated by centrifugation (a PE-6910 centrifuge, Ekokhim (Russia)), washed with distilled water to pH 7—8, and dried in a vacuum desiccator at room temperature.

Synthesis of sample Mag-2.[12] A 2 *M* NaOH solution (5 mL) was added to a solution (95 mL) containing $FeSO_4$ (1.281 g) (LenReaktiv, Russia) and KNO_3 (2.022 g) (LenReaktiv, Russia) with continuous stirring. The resulting mixture was maintained at 90 °C for 4 h, the precipitate was separated from the solution by centrifugation (8000 rpm, 15 min) and washed with distilled water until neutrality. In order to activate the surface of NPs, a 2 *M* $HClO_4$ solution (50 mL) was added to the wet magnetite precipitate, the resulting product was thoroughly mixed and maintained in a Sapfir ultrasonic bath (power was 50 W, operating frequency was 35 kHz) for 1 min. The precipitate of magnetite was separated using a permanent magnet and dried in air.

Synthesis of hybrid NPs based on sample Mag-1.[13] Dextran with M = 40 kDa was used as a stabilizer. Ammonia was added to a 10% dextran solution (15 mL) with stirring to pH 11.7, the mixture was heated to 25 °C, magnetite (0.025 g) was added, and the obtained product was vigorously stirred for 30 min. The resulting mixture was centrifuged for 20 min at a rate of 10000 rpm to precipitate large aggregates. An aliquot (0.1 mL) containing small particles of magnetite coated with a dextran shell was collected from the centrifugate. This solution was mixed with water (8.9 mL), and a solution of reducing agent (1% hydroxylamine hydrochloride (1 mL), 0.05 *M* sodium tetrahydroborate (0.1 mL), or 0.5 *M* sodium citrate (2 mL)) and a 10% aqueous ammonia (0.02 mL) were added to the system to pH 9.0. A 0.006 *M* $HAuCl_4$ solution was added to the resulting mixture in portions (0.1 mL each) four times every 10 min. The hydrosol was purified by centrifuging for 6 min at 8000 rpm, the precipitate was redispersed in distilled water, once again centrifuged under the same conditions, and then once again re-dispersed in distilled water.

Synthesis of hybrid NPs based on sample Mag-2 was carried out using a modified procedure.[14] A mixture of a 0.03 *M* methionine solution (20 mL) (Methionine-L, Diaem, Russia) and freshly prepared Fe_3O_4 sol (3.5 mL) containing magnetite (25 mg) were thoroughly mixed, maintained for 30 min in an ultrasonic bath, then a 0.1 *M* $HAuCl_4$ solution (0.6 mL) was added, and finally pH 12 was reached using a 2 *M* NaOH solution. The flask with the reaction mixture was placed in a water bath and maintained with continuous stirring for 4 h at 40 °C. The obtained NPs were separated from the solution using a permanent magnet, thoroughly washed, and then re-dispersed in water (10 mL) for further study.

Sample phase composition was determined by powder X-ray diffraction on a Shimadzu XDR-600 diffractometer (CuK_α radiation), the phases were identified using the Joint Committee on Powder Diffraction Standards database.[15] Micrographs of the samples were obtained on a Hitachi 7700M electron microscope (Hitachi, Japan) at an accelerating voltage of 100 kV. Spectrophotometric study of the obtained hydrosols of NPs was carried out on a Specol 1300 spectrometer (Analytik Jena AG, Germany). The spectra were recorded in the wavelength range of 400—1000 nm in a glass cell with an optical pathlength of 1 cm. For X-ray photoelectron spectroscopy (XPS), a drop of the obtained hydrosol was dried on a pyrographite substrate in a vacuum lock chamber of a SPECS spectrometer (SPECS Gmbh, Germany) equipped with a PHOIBOS 150-MCD-9 hemispherical electron analyzer. Sample spectra were recorded upon excitation with monochromatic radiation of AlK_α ($E = 1486.6$ eV) and MgK_α ($E = 1253.6$ eV).

Results and Discussion

The magnetite phase is already quantitatively being formed at room temperature, unlike other oxide magnetic materials. Therefore, the common method of alkaline co-precipitation of iron(II) and iron(III) salts was used to obtain magnetite sample Mag-1:

$$2\,FeCl_3 + FeSO_4 + 8\,NaOH \longrightarrow$$

$$\longrightarrow Fe_3O_4\downarrow + Na_2SO_4 + 6\,NaCl + 4\,H_2O.$$

According to powder X-ray diffraction (no X-ray diffraction pattern is shown), electron microdiffraction, and transmission electron microscopy (TEM) (Fig. 1), sample Mag-1 is a pure magnetite phase (<2.53>, <1.48>, <0.96>[15]), consisting of cubic particles with sizes in the range of 5—10 nm.

Partial oxidation of iron(II) in an alkaline medium was used to obtain magnetite sample Mag-2:

$$9\,FeSO_4 + 2\,KNO_3 + 16\,NaOH \longrightarrow$$

$$\longrightarrow 3\,Fe_3O_4\downarrow + 8\,Na_2SO_4 + K_2SO_4 + 2\,NO + 8\,H_2O.$$

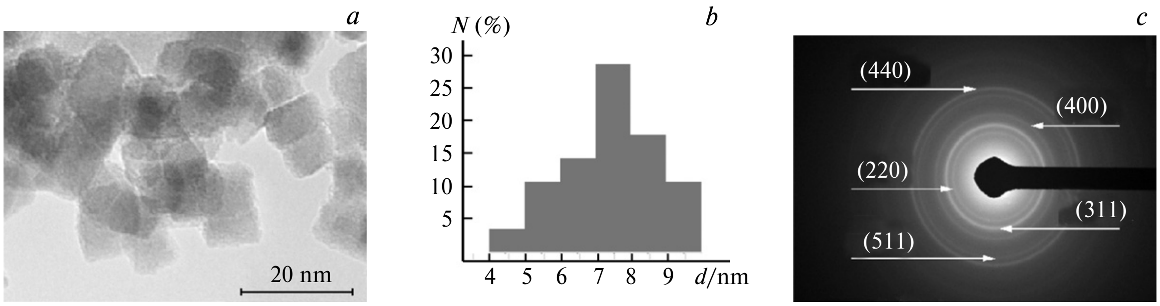

Fig. 1. TEM image (*a*), particle size distribution diagram (*b*), and electron diffraction pattern (*c*) of magnetite sample Mag-1. *N* is the fraction of particles with the indicated size (*d*).

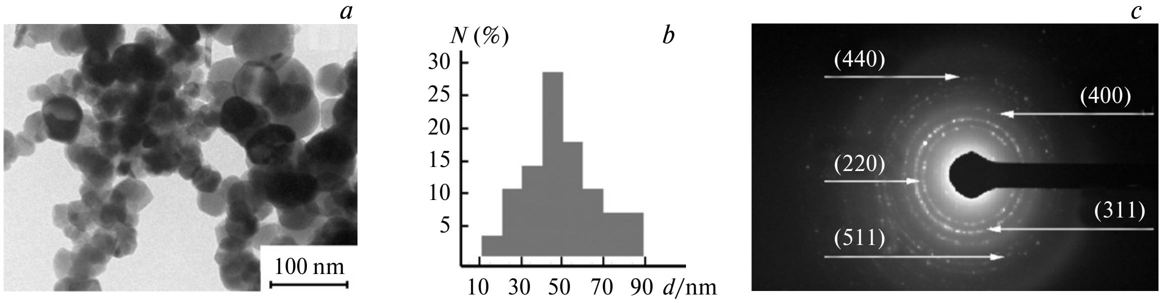

Fig. 2. TEM image (*a*), particle size distribution diagram (*b*), and electron diffraction pattern (*c*) of magnetite sample Mag-2.

Magnetite Mag-2 consists of nanoparticles with near-spherical shapes having a diameter of 50±20 nm (Fig. 2, *a*, *b*). According to electron microdiffraction, sample Mag-2 is a pure magnetite phase with a high degree of crystallinity, as indicated by reflections appearing as separate points (Fig. 2, *c*).

Hybrid particles based on magnetite Mag-1. Reduction of chloroauric acid ($HAuCl_4$) was carried out in order to obtain a gold shell on the surface of magnetite (sample Mag-1). Sodium borohydride and citrate and hydroxyamine hydrochloride were used as reducing agents of various strengths.

Sodium borohydride has a high reducing ability (potential relative to the hydrogen electrode $E^0 = -1.76$ V[16]), and was previously used in our works for the reduction of chloroauric acid in order to obtain gold NPs having various shapes.[11] However, both in these studies and in the case of sodium citrate (potential relative to the hydrogen electrode $E^0 = -0.18$ V[16]), we were not able to obtain hybrid NPs. According to transmission electron microscopy (Fig. 3), large isolated (~50 nm) gold particles were formed.

Hybrid magnetite—gold particles based on sample Mag-1 were obtained only when reducing chloroauric acid with hydroxyamine hydrochloride ($E^0_{N_2/NH_2OH\cdot H^+} = -1.87$ V[16]). According to the work,[13] hydroxylamine is adsorbed on Fe_3O_4 particles, leading to the reduction of gold not in bulk solution, but on the magnetic core surface. In this case, dextran polysaccharide molecules act as a steric stabilizer, limiting the growth of the resulting gold nanoclusters. The presence of a gold shell on the cores of sample Mag-1 was confirmed by spectrophotometric analysis of particle hydrosols magnetically separated in a constant magnetic field, washed, and re-dispersed in distilled water. The spectrum has a clear absorption maximum at 600 nm (Fig. 4, *a*). It is known from published literature[11] that hydrosols of spherical gold nanoparticles with sizes in the range of 5—10 nm have an absorption maximum at 520 nm due to surface plasmon resonance. According to the work,[17] in the case of gold nanoparticles, the shift of the SPR maximum toward the long-wavelength region is characteristic of core—shell-type structures, in which gold nanoclusters are located on the core surface. According to TEM, the obtained hybrid particles are irregularly shaped agglomerates with a diameter of 50 nm (Fig. 4, *b*). The electron microdiffraction pattern of the obtained hybrid particles (Fig. 4, *c*) contains reflections of two phases: gold and magnetite, which indicates the formation of composite nanoparticles.

Hybrid particles based on magnetite Mag-2. Magnetite—gold particles based on sample Mag-2 were obtained only when reducing chloroauric acid on the surface of Fe_3O_4

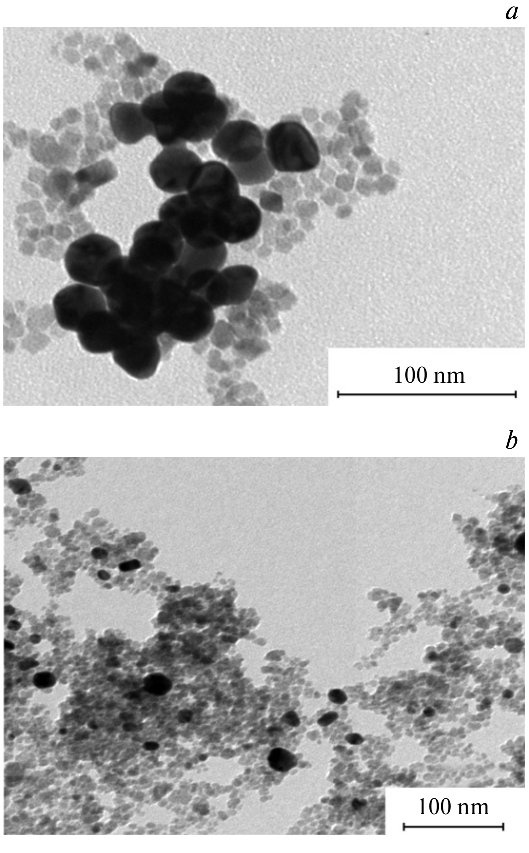

Fig. 3. TEM images of the products of the reduction of gold on the surface of magnetite Mag-1 nanoparticles using (*a*) sodium borohydride and (*b*) sodium citrate as the reducing agent.

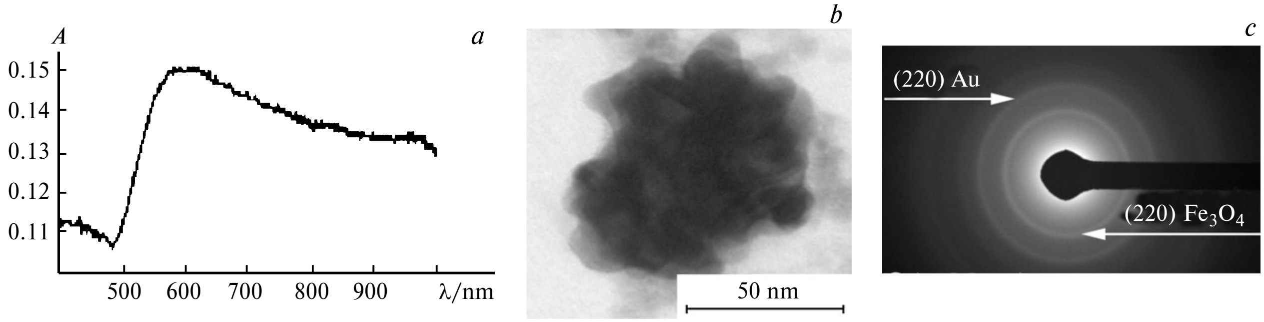

Fig. 4. Optical absorption spectrum (*a*), TEM image (*b*), and electron diffraction pattern (*c*) of hybrid nanoparticles based on magnetite (sample Mag-1) and gold.

with an amino acid, namely, L-methionine. A specific feature of this method is the iterative addition of chloroauric acid, dextran, and reducing agent until hybrid nanoparticles were obtained. This amino acid is extremely important for living organisms, because it contains a thioether group, which binds metals in the structure of many enzymes. It is a multifunctional molecule and can be used to "anchor" gold to the surface of the magnetic core. A mechanism has been proposed for binding the L-methionine molecule to gold,**[18]** according to which the amino acid forms a chelate compound due to coordination binding using nitrogen and sulfur atoms. In this case, the L-methionine carboxyl group is not involved in complexation, while it probably can participate in binding to the magnetite surface during the synthesis of hybrid NPs. The reduction of gold with methionine occurs in stages:**[19]** initially, Au^{I} is formed, which is subsequently reduced to Au^0.

A micrograph of the obtained hybrid nanoparticles shows that small (diameter of less than 1 nm) spherical gold nanoclusters are evenly distributed on the surface of magnetite (Fig. 5, *a*).

The presence of gold nanoclusters on the surface of sample Mag-2 was confirmed by XPS (Fig. 6). The presence of a strong Au 4f$_{7/2}$ line characteristic of metallic gold in the spectrum (see Fig. 6, *b*) at 84.15 eV indicates that the surface of magnetite particles is covered by Au^0 nanoclusters. The results of processing the spectra using CasaXPS software, including Shirley background subtraction and decomposition of lines using Gauss—Lorentz function, suggests a surface gold content of about 6 at.%. Nanoclusters are probably bound to the nanoparticle surface with adsorbed methionine molecules and products of its oxidation (sulfoxides and sulfones), which explains the somewhat high sulfur content in the samples (1.7 at.%). Sulfur is represented predominantly by residual methionine**[20]** (S 2p$_{3/2}$ maximum at 163.7 eV corresponds to C—S—C bond energy) (see Fig. 6, *c*). It is possible that the L-methionine sulfur atom is not bound to the surface, since no noticeable changes in the binding energy are observed compared to the isolated amino acid. Most likely, binding to the surface is accomplished through the oxygen atoms of the carboxyl group and the nitrogen atom (their binding energies are somewhat different from the individual amino acid), as suggested in the work.**[21]** However, this question requires further investigation.

A small broad maximum at 168.5 eV is characteristic of oxidized sulfur (most likely in the form of sulfonic acid

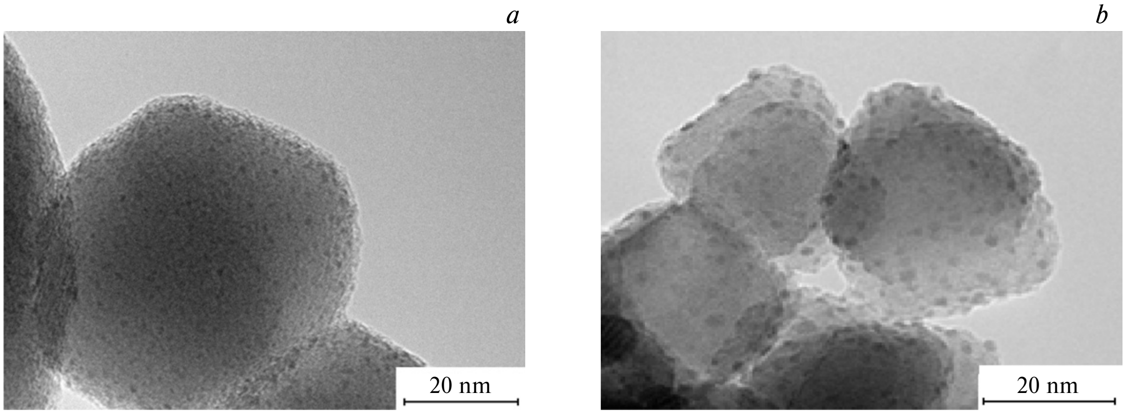

Fig. 5. TEM images of gold-containing nanoparticles based on magnetite (sample Mag-2) (*a*) single-stage coating and (*b*) three-stage reduction of Au^{III}.

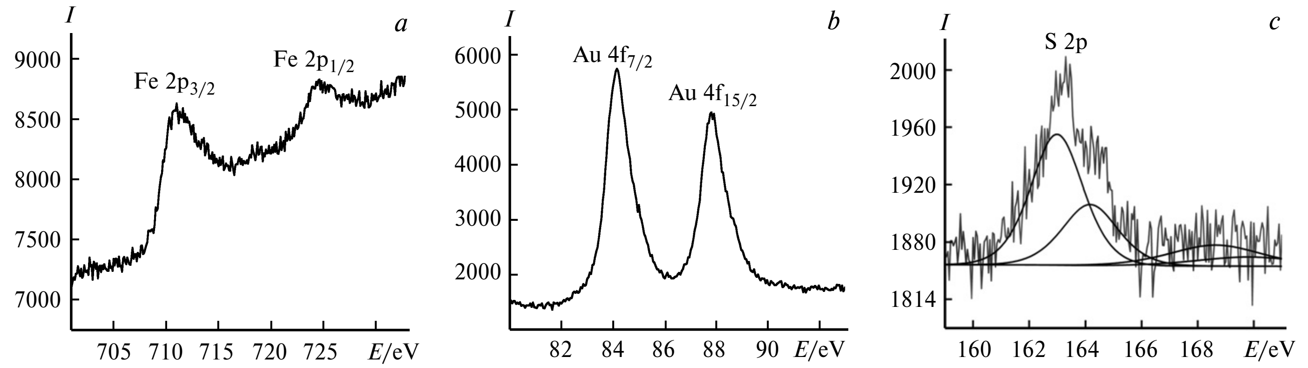

Fig. 6. XPS spectra of the Fe 2p (*a*), Au 4f (*b*), and S 2p (*c*) for the hybrid gold-containing nanoparticles based on sample Mag-2 (single-stage gold coating).

or sulfonate).[22] The weak intensity of this maximum can be related both to an excess of methionine relative to gold in the reaction mixture and to repeated washing of the obtained hybrid NPs with alcohol and water after synthesis.

In order to obtain a denser gold coating, the reduction of gold on the surface of magnetite was carried out thrice. Nanoparticles were washed with alcohol and water between iterations, but did not undergo ultrasonic treatment. According to TEM (see Fig. 5, *b*), the diameter of gold nanoclusters increased slightly, while their concentration on the surface remained almost the same. However, the sample also contained submicron gold particles, which indicated that it is impossible to obtain particles with a compact gold shell under these conditions.

The obtained hybrid NPs are magnetic nuclei decorated with gold, which can have potential applications in medicine and catalysis (in cross-coupling, hydrogenation, reduction, oxidation, cycloaddition, asymmetric synthesis reactions, *etc.*),[23,24] and serve as an intermediate when changing the growth technique during the preparation of core—shell-type nanoparticles.

In conclusion, we have studied and optimized the conditions for the synthesis of stable hydrosols of magnetic nuclei, which are magnetite nanoparticles with sizes of about 6—9 or 30—50 nm (depending on synthesis conditions). In addition, a modified method for the synthesis of hybrid nanoparticles was developed, which consisted in the simultaneous modification of the surface of the magnetic core and reduction of gold on the surface using hydrazine hydrochloride (or L-methionine). It was shown that depending on the size of the magnetic nucleus, different hybrid nanoparticles were obtained, namely, hybrid nanoparticles decorated with gold nuclei or hybrid nanoparticles of the core—shell type. All the synthesized particles were characterized by spectrophotometry, transmission electron microscopy, electron microdiffraction, and X-ray photoelectron spectroscopy. The obtained hybrid NPs can be used as promising materials for catalytic and biomedical applications.

This work was carried out using the equipment of the Krasnoyarsk Regional Center for Collective Use of the Federal Research Center "Krasnoyarsk Science Center of the Siberian Branch of the Russian Academy of Sciences".

References

1. S. Banerjee, N. P. Kumar, A. Srinivas, S. Roy, *J. Hazardous Mater.,* 2019, **375**, 216; DOI: 10.1016/j.jhazmat.2019.04.085.
2. B. Xu, H. Dou, K. Sun, J. Ding, W.Shi, X.Guo, *Langmuir,* 2011, **27**, 12134; DOI: 10.1021/la202096x.
3. S. Rajkumar, M. Prabaharan, *Colloids Surfaces, B*, 2019, **174**, 252; DOI:10.1016/j.colsurfb.2018.06.051.
4. C. Ma, H. Shao, S. Zhan, P.Hou, X. Zhang, Y. Chai, *Composite Interfaces*, 2019, **26**, 537; DOI: 10.1080/09276440.2018.1511217.
5. G. Olah, O. Faroog, G. K. S. Prakash, in *IOP Conf. Series: Materials Science and Engineering*, Institute of Physics Publishing, Majitar, 2018.
6. N. Gupta, P. Pant, C. Gupta, P. Goel, A. Jain, S. Anad, A. Pundir, *Materials Res. Innovat.*, 2018, **22**, 434; DOI: 10.1080/14328917.2017.1334846.
7. D. I. Chistyakov, T. V. Trofimova, S. V. Saykova, D. I. Saykova, *Tez. dokl. XI Mezhreg. nauchno-praktich. konf.* [*Abstracts of the XI Interregional Scientific and Practical Conference*] *(Krasnoyarsk, May 17, 2018)*, Krasnoyarskiy gos. ped. un-t, Krasnoyarsk, 2018, p. 139 (in Russian).
8. D. Chen, Q. Tang, X. Li, X. Zhou, J. Zang, W. Xue, J. Xiang, C. Guo, *Int. J. Nanomed.*, 2012, **7,** 4973; DOI: 10.2147/IJN.S35140.
9. I. V. Milto, A. Yu. Grishanova, T. K. Klimenteva, I. V. Suhodolo, G. Yu. Vasukov, V. V. Ivanova, *Biochemistry (Moscow)*, 2014, **79**, 1245; DOI: 10.1134/S0006297914110121.
10. Z. Yarjanli, K. Ghaedi, A. Esmaeili, S. Rahgozar, A. Zarrabi, *BMC Neurosci.,* 2017, **18,** 51; DOI: 10.1186/s12868-017-0369-9.
11. T. V. Trofimova, S. V. Saykova, D. I. Saykova, D. I. Chistyakov, *J. Siber. Fed. Univ. Chem.,* 2016, **9** (4), 496; DOI: 10.17516/1998-2836-2016-9-4-496-503.
12. I. Y. Goon, L. M. H. Lai, M. Lim, P. Munroe, J. J. Gooding, R. Amal, *Chem. Mater.*, 2009, **21**, 673; DOI: 10.1021/cm8025329.
13. L. L. Ma, M. D. Feldman, J. M. Tam, A. S. Paranjape, K. K. Cheruku, T. A. Larson, J. O. Tam, D. R. Ingram,

V. Paramita, J. W. Vilard, J. T. Jenkins, T. Wang, G. D. Clarke, R. Asmis, K. Sokolov, B. Chandrasekar, T. E. Milner, K. P. Johnston, *ACS Nano*, 2009, **3**, 2686; DOI: 10.1021/nn900440e.

14. A. Mikalauskaite, G. Niaura, R. Kondrotas, A. Jagminas, *J. Phys. Chem.*, 2015, **119**, 17398; DOI: 10.1021/acs.jpcc.5b03528.
15. *Powder Diffraction File JCPDS, Version 33*, 2018.
16. T. Pal, S. De, N. R. Jana, N. Pradhan, R. Mandal, A. Pal, *Langmuir*, 1998, **14**, 4724; DOI: 10.1021/la980057n.
17. Yu. Yu. Lur´e, *Spravochnik po analiticheskoy khimii* [*Handbook of Analytical Chemistry*], Khimiya, Moscow, 1989, 448 p. (in Russian).
18. A. V. Vujačić, J. Z. Savića, S. P. Soviljb, K. Mészáros Szécsényic, N. Todorovićd, M. Ž. Petkovića, V. M. Vasića, *Polyhedron*, 2009, **28**, 593; DOI: 10.1016/j.poly.2008.11.045.
19. J. D. Atwood, in *Inorganic and Organometallic Reaction Mechanisms*, VCH Publishers, New York, 1997, pp. 312.
20. R. A. Brizzolara, *Surface Sci. Spectr.*, 1996, **4**, 96; DOI: 10.1116/1.1247810.
21. L. Thomsen, M. T. Wharmby, D. P. Riley, G. Held, M. J. Gladys, *Surface Sci.*, 2009, **603**, 1253; DOI: 10.1016/j.susc.2009.03.014
22. P. Gobbo, M. C. Biesinger, M. S. Workentin, *Chem. Commun.*, 2013, **49**, 2831; DOI: 10.1039/C3CC00050H.
23. M. B. Gawande, P. S. Branco, R. S. Varma, *Chem. Soc. Rev.*, 2013, **42**, 3371; DOI: 10.1039/C3CS35480F.
24. S. Roy, M. A. Pericas, *Org. Biomolec. Chem.*, 2009, **7**, 2669; DOI: 10.1039/B903921J.

Received October 1, 2019;
in revised form March 19, 2020;
accepted March 29, 2020